

Article

# Ammonium-Nitrogen ( $\text{NH}_4^+\text{-N}$ ) Removal from Groundwater by a Dropping Nitrification Reactor: Characterization of $\text{NH}_4^+\text{-N}$ Transformation and Bacterial Community in the Reactor

Amit Kumar Maharjan <sup>1</sup>, Tatsuru Kamei <sup>2,3</sup>, Iswar Man Amatya <sup>4</sup>, Kazuhiro Mori <sup>3</sup>, Futaba Kazama <sup>3</sup> and Tadashi Toyama <sup>3,\*</sup>

<sup>1</sup> Integrated Graduate School of Medicine, Engineering and Agricultural Sciences, University of Yamanashi, Yamanashi 400-8511, Japan; g17dea01@yamanashi.ac.jp or amit\_kmr@hotmail.com

<sup>2</sup> School of Allied Health Sciences, Kitasato University, Kanagawa 252-0373, Japan; tkamei@kitasato-u.ac.jp

<sup>3</sup> Graduate Faculty of Interdisciplinary Research, University of Yamanashi, Yamanashi 400-8511, Japan; mori@yamanashi.ac.jp (K.M.); kfutaba@yamanashi.ac.jp (F.K.)

<sup>4</sup> Department of Civil Engineering, Pulchowk Campus, Institute of Engineering, Tribhuvan University, Lalitpur 44700, Nepal; iswar@ioe.edu.np

\* Correspondence: ttohyama@yamanashi.ac.jp

Received: 21 November 2019; Accepted: 20 February 2020; Published: 22 February 2020



**Abstract:** A dropping nitrification reactor was proposed as a low-cost and energy-saving option for the removal of  $\text{NH}_4^+\text{-N}$  from contaminated groundwater. The objectives of this study were to investigate  $\text{NH}_4^+\text{-N}$  removal performance and the nitrogen removal pathway and to characterize the microbial communities in the reactor. Polyolefin sponge cubes (10 mm × 10 mm × 10 mm) were connected diagonally in a nylon thread to produce 1 m long dropping nitrification units. Synthetic groundwater containing 50 mg L<sup>-1</sup>  $\text{NH}_4^+\text{-N}$  was added from the top of the hanging units at a flow rate of 4.32 L day<sup>-1</sup> for 56 days. Nitrogen-oxidizing microorganisms in the reactor removed 50.8–68.7% of the  $\text{NH}_4^+\text{-N}$  in the groundwater, which was aerated with atmospheric oxygen as it flowed downwards through the sponge units. Nitrogen transformation and the functional bacteria contributing to it were stratified in the sponge units. *Nitrosomonadales*-like AOB predominated and transformed  $\text{NH}_4^+\text{-N}$  to  $\text{NO}_2^-\text{-N}$  in the upper part of the reactor. *Nitrospirales*-like NOB predominated and transformed  $\text{NO}_2^-\text{-N}$  to  $\text{NO}_3^-\text{-N}$  in the lower part of the reactor. The dropping nitrification reactor could be a promising technology for oxidizing  $\text{NH}_4^+\text{-N}$  in groundwater and other similar contaminated wastewaters.

**Keywords:**  $\text{NH}_4^+\text{-N}$  removal; groundwater; dropping nitrification; ammonia-oxidizing bacteria; nitrite-oxidizing bacteria; polyolefin sponge

## 1. Introduction

Groundwater, an important source of domestic drinking water, poses serious environmental and public health concerns when contaminated by pollutants such as ammonium-nitrogen ( $\text{NH}_4^+\text{-N}$ ). Other contaminants include arsenic as well as microorganisms such as *Giardia*, *Campylobacter*, *Cryptosporidium*, *Salmonella*, and *Escherichia coli*.  $\text{NH}_4^+\text{-N}$  groundwater contamination is usually caused by anthropogenic activities [1–5]. Groundwater  $\text{NH}_4^+\text{-N}$  levels of ≤ 120 mg L<sup>-1</sup>, 69.8 mg L<sup>-1</sup>, 10 mg L<sup>-1</sup>, and 120 mg L<sup>-1</sup> have been reported for Australia [6], Vietnam [7], China [8], and the Kathmandu valley of Nepal [9], respectively. These concentrations can vary temporally in areas of intensive groundwater/surface water interactions [1]. The threshold proposed in the World Health

Organization (WHO) guideline for drinking water of  $1.5 \text{ mg L}^{-1}$  [10] is substantially less than the levels for these different locations. High  $\text{NH}_4^+\text{-N}$  levels in water supplies lead to unpleasant odors and taste. These high levels are a major cause for reducing the disinfection efficacy of chlorine and other halogens, as well as increasing the risk of pathogen contamination during water treatment and distribution; hence, the levels of  $\text{NH}_4^+\text{-N}$  in groundwater must be decreased before consumption.

The in situ permeable reactive barrier (PRB) is a promising groundwater  $\text{NH}_4^+\text{-N}$  removal technology. Several laboratory- and full-scale PRBs have effectively removed  $\text{NH}_4^+\text{-N}$  from groundwater [6,8,11–13]. Although a PRB is cost-effective in the long term, it, nonetheless, requires large-scale construction and incurs a high initial cost [14]. Therefore, low-cost, energy-sparing, simple, and compact alternative technologies are needed to remove groundwater  $\text{NH}_4^+\text{-N}$ , particularly in developing countries and small rural communities.

In the present study, a dropping nitrification reactor was proposed for the removal of  $\text{NH}_4^+\text{-N}$  from contaminated groundwater (Figure S1). This configuration simulated a down-flow hanging sponge (DHS) system. The DHS system is a low-cost, energy-saving option that is simple in construction and easy in operation and maintenance compared to the PRB. The DHS reactor was originally developed for the treatment of domestic sewage. DHS systems efficiently reduce organic compounds, chemical oxygen demand (COD), biochemical oxygen demand (BOD), and nitrogen in sewage [15–20]; they have also been used for the treatment of several kinds of industrial wastewater and for various other purposes [21]. The DHS reactor is a trickling filter using polyurethane sponge as the microbial carrier. Wastewater trickles down from the top of the sponge under the influence of gravity. In the down-flow process, wastewater is exposed to oxygen in the air; thus, this reactor does not require any external aeration [17,22,23]. The organic compounds and  $\text{NH}_4^+\text{-N}$  in wastewater can be oxidized by the microorganisms on the surface and in the interior of the sponge. During DHS wastewater treatment and other biological nitrogen removal processes,  $\text{NH}_4^+\text{-N}$  is subjected to ammonia-oxidizing bacteria (AOB) that generate nitrite-nitrogen ( $\text{NO}_2^-\text{-N}$ ). The latter, in turn, is oxidized to nitrate-nitrogen ( $\text{NO}_3^-\text{-N}$ ) by nitrite-oxidizing bacteria (NOB) [22]. To the best of our knowledge, however, no prior study has investigated the application of DHS for the treatment of  $\text{NH}_4^+\text{-N}$ -contaminated groundwater containing little or no organic carbon. Here, we hypothesized that a dropping nitrification reactor can effectively remove  $\text{NH}_4^+\text{-N}$  from contaminated groundwater. This reactor will be a low-cost, low-energy consuming, easily operable, and environmentally friendly option for  $\text{NH}_4^+\text{-N}$  removal from groundwater.

The aims of this study were to test the potential of the dropping nitrification reactor for the removal of  $\text{NH}_4^+\text{-N}$  from contaminated groundwater to elucidate the single axis, top-to-bottom nitrogen removal pathway and to identify the characteristics of the microbial community, including AOB and NOB in the reactor.

## 2. Materials and Methods

### 2.1. Synthetic $\text{NH}_4^+\text{-N}$ -Contaminated Groundwater

Synthetic  $\text{NH}_4^+\text{-N}$ -contaminated ( $50 \text{ mg L}^{-1} \text{ NH}_4^+\text{-N}$ ) groundwater ( $104.5 \text{ mg Na}_2\text{HPO}_4 \cdot 12\text{H}_2\text{O}$ ,  $17 \text{ mg KH}_2\text{PO}_4$ ,  $37.5 \text{ mg NaCl}$ ,  $17.5 \text{ mg KCl}$ ,  $23 \text{ mg CaCl}_2 \cdot 2\text{H}_2\text{O}$ ,  $25.6 \text{ mg MgSO}_4 \cdot 7\text{H}_2\text{O}$ ,  $236 \text{ mg (NH}_4)_2\text{SO}_4$ , and  $353 \text{ mg of NaHCO}_3$  per L tap water;  $\text{pH } 8.0 \pm 0.1$ ) was prepared for this study. The constituents and their concentrations in the synthetic groundwater were determined based on the chemical composition of  $\text{NH}_4^+\text{-N}$ -contaminated groundwater sampled from the Kathmandu Valley [24].

### 2.2. Setup of the Laboratory-Scale Dropping Nitrification Reactor

Polyolefin sponges ( $10 \text{ mm} \times 10 \text{ mm} \times 10 \text{ mm}$ ; Sekisui Aqua Systems Company, Osaka, Japan) served as the medium for the reactor. Polyolefin sponges are superior to polyurethane sponges in DHS (more durable, firmer shape, and higher load bearing capacity). Approximately 82 sponge cubes were connected diagonally in a nylon thread to form a hanging sponge unit with an effective length of 1 m (Figure S1) and a dry weight of approximately 2.94 g. The sponge units were incubated with

10 L of a synthetic  $\text{NH}_4^+$ -N-contaminated groundwater mixed with the activated sludge (10:1, v/v). The activated sludge from a municipal wastewater treatment plant in Kofu, Yamanashi, Japan, served as the bacterial inoculum for the sponge units. The suspension was aerated with a pump at a flow rate of  $1 \text{ L min}^{-1}$  for 10 days before setting up the reactor to establish microbial communities in the sponge media. A laboratory-scale reactor was prepared using a stainless-steel frame (1.2 m width, 0.45 m depth, 1.5 m height) and set up in a greenhouse at the University of Yamanashi, Kofu, Yamanashi, Japan. The reactor consisted of four separate hanging sponge units (Figure S1). The reactor was covered with a sun-shielding sheet to prevent microalgal growth.

### 2.3. Operating Conditions of the Laboratory-Scale Dropping Nitrification Reactor

The groundwater  $\text{NH}_4^+$ -N removal reactor was operated for 56 days. The contaminated groundwater was fed on the top of each hanging sponge unit at a flow rate of  $4.32 \text{ L day}^{-1}$  ( $3 \text{ mL min}^{-1}$ ). Water samples were collected from the influent (0 m from the top of the unit), effluent (1 m from the top), and at intermediate sampling points (0.25, 0.50, and 0.75 m from the top) to monitor  $\text{NH}_4^+$ -N,  $\text{NO}_2^-$ -N, and  $\text{NO}_3^-$ -N concentrations. Influent and effluent samples were collected to measure water temperature, pH, redox potential (ORP), and dissolved oxygen (DO) every day or every alternate day. The sponge material was sampled at 0.00, 0.25, 0.50, 0.75, and 1.00 m from the top of the unit every 2 weeks for microbial community analyses.

### 2.4. Physicochemical Parameters and Nitrogen Concentration in Water Samples

Water temperature, pH, ORP, and DO of the influent and effluent samples were measured on-site with a pH/Temp meter (AS600, AS ONE Corporation, Osaka, Japan), a waterproof ORP meter (ORP-6041, Custom Corp., Chiyoda-ku, Japan), and a DO meter (PDO-520, Fuso Inc., Chuo-ku, Japan), respectively.

Before determining the nitrogen concentration, water samples were filtered through a membrane filter (polypropylene,  $0.45 \mu\text{m}$  pore size; Membrane Solutions Co. Ltd., Minato-ku, Japan).  $\text{NH}_4^+$ -N,  $\text{NO}_2^-$ -N, and  $\text{NO}_3^-$ -N concentrations were measured in accordance with the Standard Methods for the Examination of Water and Wastewater [25]. The indophenol method was used to determine  $\text{NH}_4^+$ -N concentration, and the *N*-(1-naphthyl) ethylenediamine and UV adsorption (220 and 275 nm) methods were used to determine  $\text{NO}_2^-$ -N and  $\text{NO}_3^-$ -N concentrations, respectively.

### 2.5. Kinetics of $\text{NH}_4^+$ -N Removal Along the Single Axis of the Dropping Nitrification Reactor

The  $\text{NH}_4^+$ -N profiles along the single axis of the reactor from the top (influent, 0 m) to the bottom (effluent, 1 m) were evaluated according to zero- and first-order kinetic reactions as shown in Equations (1) and (2), respectively:

$$\frac{dC}{dt} = -k_0 \times C^0 = -k_0 \quad (1)$$

$$\frac{dC}{dt} = -k_1 \times C^1 = -k_1 \times C \quad (2)$$

where  $C$  is the  $\text{NH}_4^+$ -N concentration,  $\frac{dC}{dt}$  is the rate of change in  $\text{NH}_4^+$ -N concentration per unit time, and  $k_0$  and  $k_1$  are the zero- and the first-order kinetic rate constants, respectively.

### 2.6. DNA Extraction from Sponge Samples and Quantification of Functional Microbial Genes

The sponge samples (approximately 100 mg wet weight = approximately 7.6 mg dry weight) were cut from the corners of the sponges and used for the microbial community analyses. Microbial DNA was extracted from the sponge samples with NucleoSpin Tissue (MACHEREY-NAGEL GmbH, Duren, Germany) according to the manufacturer's protocol.

Bacterial 16S rRNA and the ammonia monooxygenase (*amoA*), nitrite oxidoreductase (*nxrA*), and nitrite reductase (*nirK* and *nirS*) genes were quantified by real-time quantitative polymerase chain

reaction (RT-qPCR) based on functional gene-targeted primer sets (Table S1) in a Thermal Cycler Dice Real-Time System II (TaKaRa Bio Inc., Shiga, Japan). Each qPCR assay was conducted in a 25  $\mu$ L reaction mixture including 12.5  $\mu$ L SYBR Premix Ex Taq (TaKaRa Bio, Shiga, Japan), 0.5  $\mu$ M of each forward and reverse primer (Table S1), 2  $\mu$ L template DNA, and 9.5  $\mu$ L deionized H<sub>2</sub>O. The reaction conditions were as follows: initial denaturation by preheating at 95 °C for 30 s, 40 cycles of 98 °C for 5 s, annealing at the specified temperatures (which varied with primer type; Table S1) for 50 s, and an extension at 72 °C for 1 min, followed by a dissociation stage (95 °C for 15 s, 60 °C for 30 s, and 95 °C for 15 s). A standard curve was plotted for each gene using a synthetic plasmid carrying the target sequence. All qPCRs were conducted in duplicate. The gene abundances in the nitrification unit (copies per unit) were calculated using the gene abundances in the sponge material (copies per mg) and the total weight of sponge materials in the unit (mg per unit).

### 2.7. Phylogenetic Analysis of the Bacterial Community

The extracted bacterial DNA samples were subjected to Illumina MiSeq 16S rRNA gene sequencing (Illumina, San Diego, CA, USA). The V4 region of the 16S rRNA gene was amplified by PCR with the universal primers 515F (5'-Seq A-TGT-GCC-AGC-MGC-CGC-GGT-AA-3') and 806R (5'-Seq B-GGA-CTA-CHV-GGG-TWT-CTA-AT-3'). PCR amplicons were sequenced in an Illumina MiSeq Sequencer (Illumina, San Diego, CA, USA). Sequence reads were analyzed with Sickle v. 1.33 (<https://github.com/najoshi/sickle>), Fastx Toolkit v. 0.0.13.2 ([http://hannonlab.cshl.edu/fastx\\_toolkit/download.html](http://hannonlab.cshl.edu/fastx_toolkit/download.html)), FLASH v. 1.2.10 (<https://sourceforge.net/projects/flashpage/files/>), and USEARCH v. 8.0.1623\_i86linux64 (<https://www.drive5.com/usearch/>). In these analyses, contigs were formed, and error sequences and chimeras were removed. All operational taxonomic units (OTUs) were clustered at a cutoff of 0.03 (97% similarity). OTUs with < 1% relative abundance among all sequences in all samples were summed as "others". Sequencing and sequence-read analyses were conducted at FASMAC (Kanagawa, Japan).

### 2.8. Statistical Analysis

The mean and standard deviation of the physicochemical parameters and nitrogen concentrations were calculated from the data of four replicates of 1 m long dropping nitrification units. Gene abundances ( $\pm$  SD) were calculated using duplicate experiments for each sample. A *t*-test was used to compare the pairs of groups for significant differences ( $P < 0.05$ ). The data were processed in SPSS v. 20 (IBM Corp., Armonk, NY, USA).

## 3. Results and Discussion

### 3.1. Changes in Physicochemical Parameters

Changes in pH, ORP, and DO in the influent and effluent samples over 56 days of experimentation are shown in Figure 1. Water temperature in the influent and effluent samples ranged from 22 to 32 °C. The pH of the influent was  $8.0 \pm 0.1$  and that of the effluent ranged from 5.7 to 7.4. The pH of the effluent was significantly lower ( $P < 0.05$ ) than that of the influent. The pH decrement from the top to the bottom of the reactor indicated that H<sup>+</sup> ion was released (acidification) as a result of microbial nitrification [26,27].

The ORP measurements in the influent and effluent samples were in the ranges of 109–155 and 127–174, respectively. The DO measurements in the influent and effluent samples were in the ranges of 6.0–8.3 and 6.5–8.5, respectively. The ORP and DO after 1 week of operation were significantly higher ( $P < 0.05$ ) in the effluent than in the influent. Groundwater was fed from the top to the bottom of the reactor. During downward flow, oxygen diffusion into the groundwater from the air caused an increase in the DO concentration in the groundwater. Similar results have been obtained in the DHS reactors treating anaerobic wastewater [19,28,29]. Elevated DO levels are favorable for microbial nitrification [28].

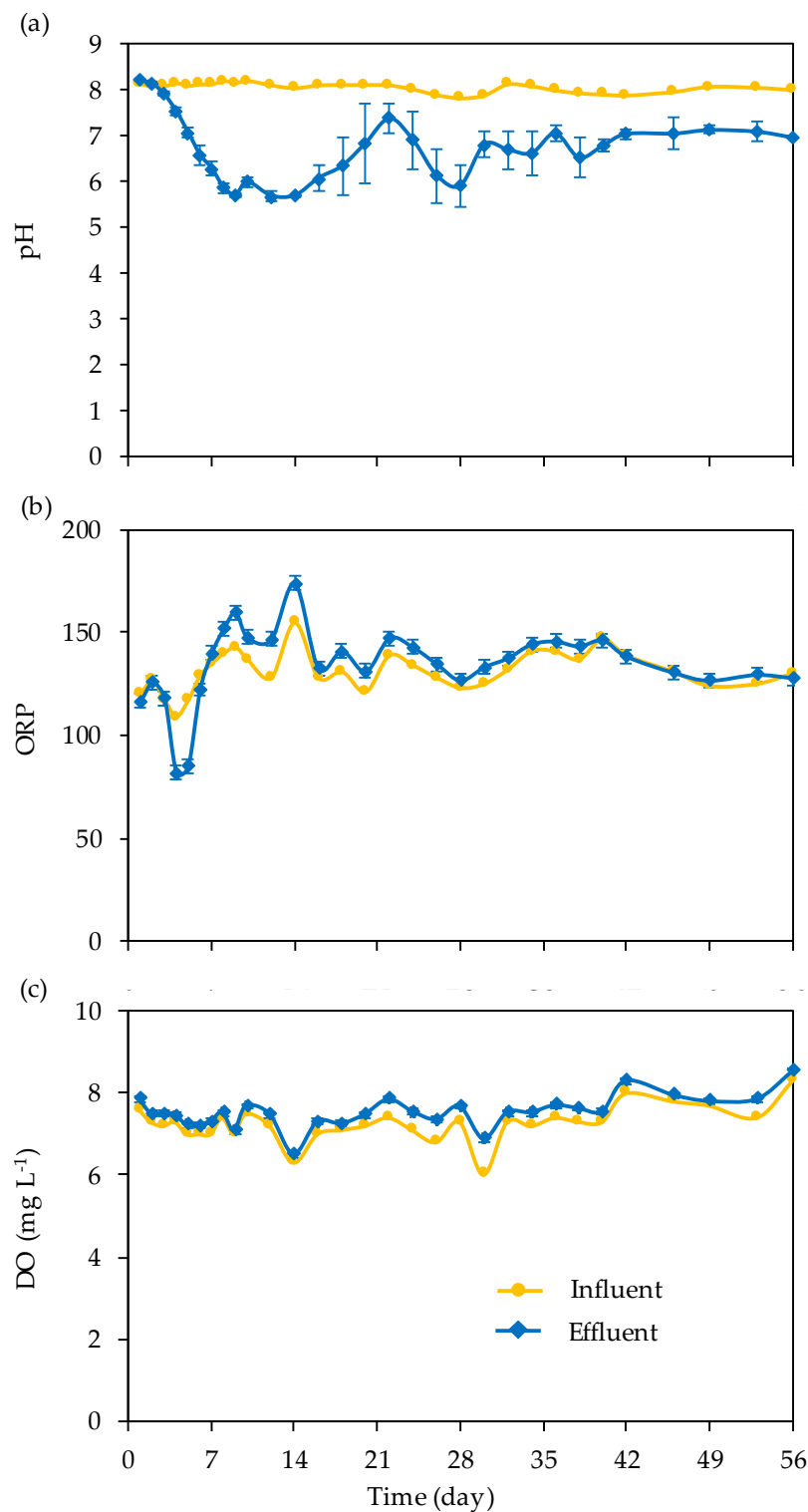


**Figure 1.** Changes in pH (a), redox potential (ORP) (b), and dissolved oxygen (DO) (c) in the influent and effluent samples over 56 days of operation. Effluent values are means  $\pm$  SD ( $n = 4$ ).

### 3.2. Removal Efficiency of $\text{NH}_4^+\text{-N}$ and Nitrogen Transformations in the Dropping Nitrification Reactor

Changes in  $\text{NH}_4^+\text{-N}$ ,  $\text{NO}_2^-\text{-N}$ , and  $\text{NO}_3^-\text{-N}$  in the influent and effluent samples over 56 days of experimentation are shown in Figure 2. The  $\text{NH}_4^+\text{-N}$  concentration in the effluent gradually decreased after initiating operation, reached steady state after 1 week of operation, and then stabilized in the range of 15.0–25.2 mg L<sup>-1</sup> (50.8–68.7%  $\text{NH}_4^+\text{-N}$  removal). The reactors achieved a  $\text{NH}_4^+\text{-N}$  removal

steady state within a short period of operation. The total inorganic nitrogen ( $\text{NH}_4^+\text{-N}$ ,  $\text{NO}_2^-\text{-N}$ , and  $\text{NO}_3^-\text{-N}$ ) in the effluent samples was approximately the same as the influent  $\text{NH}_4^+\text{-N}$  concentration after 3 days of operation. The decrease in  $\text{NH}_4^+\text{-N}$  concentration from the influent to the effluent was equivalent to the increase in the  $\text{NO}_2^-\text{-N}$  and  $\text{NO}_3^-\text{-N}$  concentrations in the effluent where the latter two compounds accumulated; thus,  $\text{NH}_4^+\text{-N}$  removal was caused exclusively by biological nitrification in which  $\text{NH}_4^+\text{-N}$  was oxidized to  $\text{NO}_2^-\text{-N}$  and  $\text{NO}_3^-\text{-N}$ . Ammonia volatilization was not significant in the reactor, because pH value was  $< 9.3$  in the synthetic groundwater [30]. For up to 35 days, the  $\text{NO}_2^-\text{-N}$  concentration was higher than the  $\text{NO}_3^-\text{-N}$  concentration in the effluent. Notably, after 35 days, the opposite trend was observed; therefore, the oxidation of  $\text{NH}_4^+\text{-N}$  to  $\text{NO}_2^-\text{-N}$  was effective and fast after starting operation of the reactor when compared to the oxidation of  $\text{NO}_2^-\text{-N}$  to  $\text{NO}_3^-\text{-N}$ .

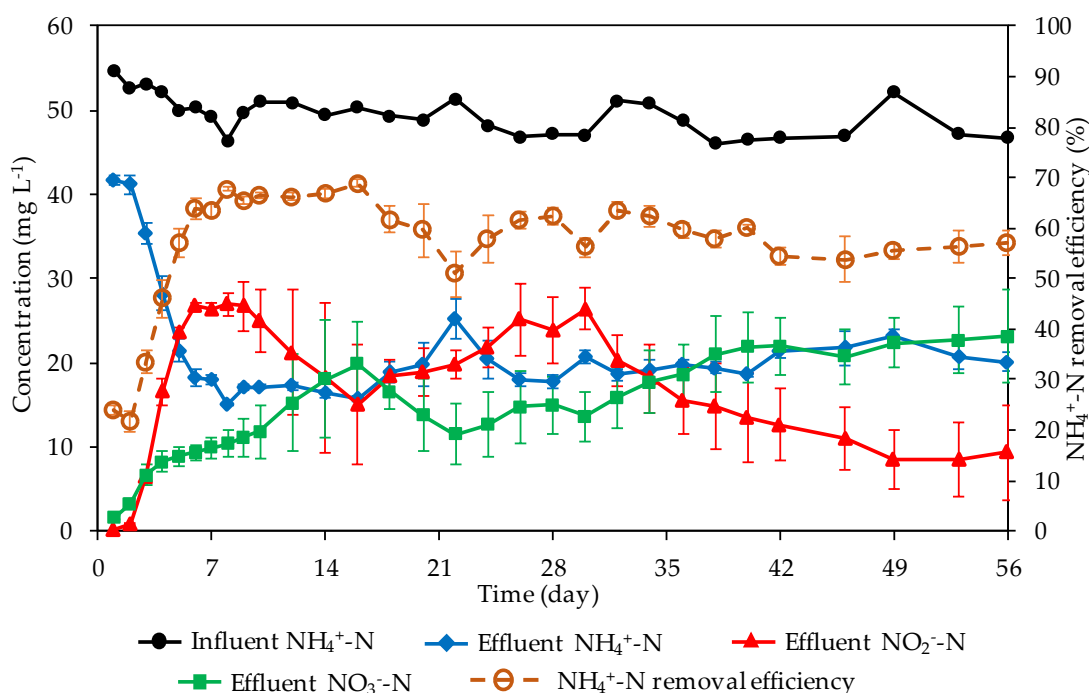


**Figure 2.** Changes in  $\text{NH}_4^+\text{-N}$ ,  $\text{NO}_2^-\text{-N}$ , and  $\text{NO}_3^-\text{-N}$  concentration and  $\text{NH}_4^+\text{-N}$  removal efficiency over 56 days of operation. Values are means  $\pm$  SD ( $n = 4$ ).

### 3.3. Variations in the Abundances of the Functional Microbial Genes Involved in the Nitrogen Transformations

The abundances of bacterial 16S rRNA, *amoA*, *nxrA*, *nirK*, and *nirS* in the reactor over 56 days of operation are shown in Figure 3. The bacterial 16S rRNA gene abundance ranged from  $8.2 \times 10^{12}$  to  $4.5 \times 10^{13}$  copies per unit. The abundance of *amoA* significantly increased ( $P < 0.05$ ) from  $1.5 \times 10^{10}$  to  $3.3 \times 10^{11}$  copies per unit within the initial 14 days and then reached and maintained a peak at  $5.5 \times 10^{11}$  copies per unit. The abundance of *nxrA* gradually and steadily increased from  $5.2 \times 10^7$  to  $1.3 \times 10^{12}$  copies per unit over 56 days; thus, the AOB population and activity increased faster in the reactor than those of NOB. These changes in *amoA* and *nxrA* abundance corresponded to the changes in  $\text{NH}_4^+\text{-N}$ ,  $\text{NO}_2^-\text{-N}$ , and  $\text{NO}_3^-\text{-N}$  concentration in the effluent (Figure 2). The AOB population should be larger than that of the NOB in balanced nitrifying systems [31,32]. The NOB population was smaller than the AOB population in wastewater treatment systems, such as in sequencing batch reactors [33] and in combined activated sludge-rotating biological contactor and anaerobic-anoxic-oxide (A2O) processes [34]. NOB growth is relatively slow in the absence of nitrite [35]. Similar to these previous reports, the AOB population increased more quickly in this reactor after the onset of the operation compared to the NOB population.

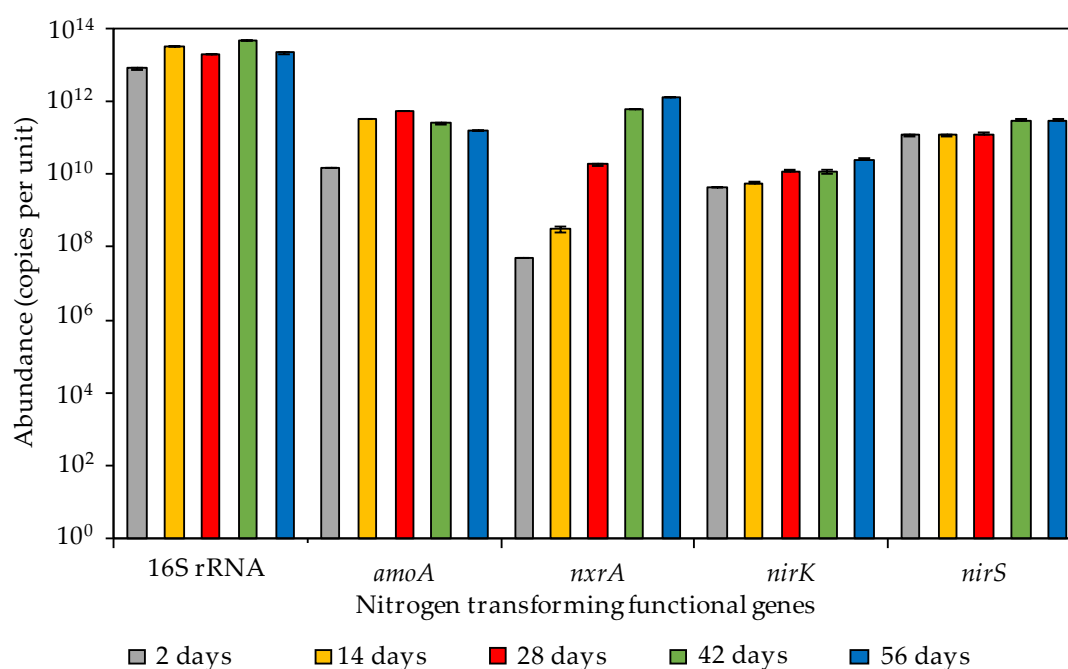


**Figure 3.** Changes in the abundances of 16S rRNA, *amoA*, *nxrA*, *nirK*, and *nirS* in the dropping nitrification units over 56 days of operation. Average numbers of gene copies  $\pm$  SD are shown for duplicate experiments.

In contrast, the abundances of *nirK* and *nirS* were  $4.3 \times 10^9$ – $2.6 \times 10^{10}$  and  $1.2 \times 10^{11}$ – $3.1 \times 10^{11}$  copies per unit, respectively, and did not change significantly over 56 days. Functional denitrification genes (*nirK* and *nirS*) were detected in the sponge media. Nevertheless, no denitrification was observed in this experiment as the reactor was highly aerobic (Figure 1c) and the organic carbons (i.e., electron donors) for heterotrophic denitrification were not included in the synthetic groundwater.

### 3.4. $\text{NH}_4^+$ -N, $\text{NO}_2^-$ -N, and $\text{NO}_3^-$ -N Concentration and Functional N-Transformation Gene Profiles along the Single Axis of the Dropping Nitrification Reactor

The biweekly  $\text{NH}_4^+$ -N,  $\text{NO}_2^-$ -N, and  $\text{NO}_3^-$ -N concentrations and the abundances of the functional bacterial genes (bacterial 16S rRNA, *amoA*, *nxrA*, *nirK*, and *nirS*) along the single axis of the nitrification units (from the top (influent) to the bottom (effluent; 1 m)) are shown in Figure 4. The  $\text{NH}_4^+$ -N concentration rapidly decreased from the top (0 m) to the middle (0.25–0.75 m) of the nitrification reactor. The  $\text{NO}_2^-$ -N concentration sharply increased from the top to the middle and then decreased gradually. The  $\text{NO}_3^-$ -N concentration gradually increased from the top to the bottom of the sponge units. The abundance of *amoA* was higher at the top than at the bottom. In contrast, the abundance of *nxrA* in the sponge units after 14 days of operation was higher in the middle to the bottom parts than in the top (Figure 4). Ammonium oxidation almost occurred in the upper parts, while nitrite oxidation almost occurred from the middle to the bottom of the units.

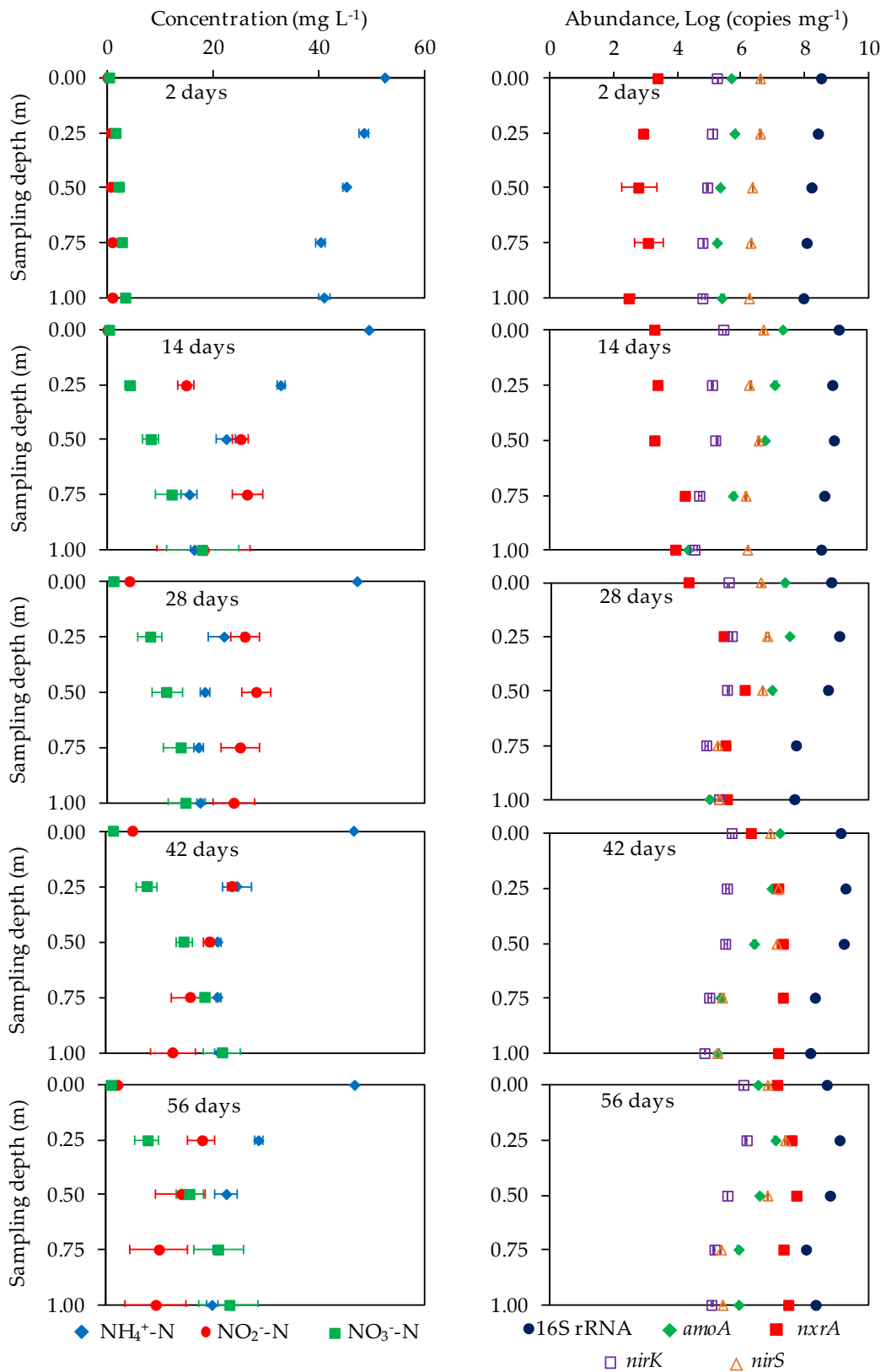


**Figure 4.** Profiles of NH<sub>4</sub><sup>+</sup>-N, NO<sub>2</sub><sup>-</sup>-N, NO<sub>3</sub><sup>-</sup>-N, and functional genes along the single axis of the dropping flow every 2 weeks. NH<sub>4</sub><sup>+</sup>-N, NO<sub>2</sub><sup>-</sup>-N, and NO<sub>3</sub><sup>-</sup>-N concentrations indicated are the averages ± SD of four replicate reactors. The gene copies shown represent the averages ± SD of duplicate experiments.

The decrease in  $\text{NH}_4^+\text{-N}$  concentration along the single axis of the nitrification units more nearly approximated a first-order than a zero-order kinetic reaction (Figure S2). The first-order kinetic constant ( $k_1$ ) significantly increased ( $P < 0.05$ ) from 0.35 to  $1.55 \text{ m}^{-1}$  within the first 14 days and then ranged from 1.01 to  $1.28 \text{ m}^{-1}$  (Figure 5). The first-order kinetic constant for the increase in  $\text{NH}_4^+\text{-N}$  removal within the initial 14 days corresponded to the increase in *amoA* gene abundance (Figure 3).

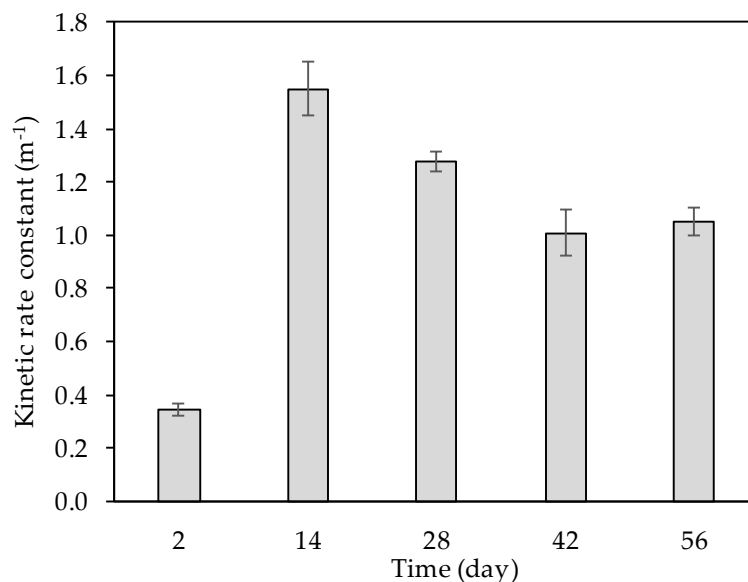


**Figure 5.** First-order kinetic constant ( $k_1$ ) for the decrease in  $\text{NH}_4^+\text{-N}$  concentration along the single axis of the dropping nitrification reactor over 56 days of operation. Values are means  $\pm$  SD ( $n = 4$ ).

### 3.5. Bacterial Community Structure Profiles along the Single Axis of the Dropping Nitrification Reactor

Bacterial community compositions at the class and order levels along the single axis of the reactor on the 56th day are shown in Figure 6. At the class level, *Betaproteobacteria* (37.9% of all classes), *Alphaproteobacteria* (24.2%), and *Gammaproteobacteria* (17.2%) predominated at the top of the nitrification reactor, whereas *Alphaproteobacteria* (16.2%), *Betaproteobacteria* (15.1%), and *Nitrospira* (NOB class; 25.6%) predominated at the bottom.

At the order level, *Nitrosomonadales* (AOB order; 34.5%) and *Xanthomonadales* (16.6%) predominated at the top of the nitrification unit; however, their abundances decreased to 11.4% and 7.3%, respectively, at the bottom part. On the other hand, the abundance of *Nitrospirales* (NOB order) increased along with the downward flow starting from the middle and reached 25.7% at the bottom of the unit. *Nitrosomonas* spp. (*Nitrosomonadales*) and *Nitrospira* spp. (*Nitrospirales*) were the dominant AOB and NOB species, respectively, in aerobic biological wastewater treatment plants [36] and DHS systems [37]. *Nitrosomonadales* and *Nitrospirales* members were also detected in the nitrification units of the present study. Moreover, the abundance of *Nitrosomonadales*-like AOB was relatively higher in the upper part, while the abundance of *Nitrospirales*-like NOB was higher in the lower part of the nitrification units. These spatial differences in AOB and NOB along the single axis of the nitrification unit were consistent with the profiles for the  $\text{NH}_4^+\text{-N}$ ,  $\text{NO}_2^-\text{-N}$ , and  $\text{NO}_3^-\text{-N}$  concentrations and the abundances of *amoA* and *nxA* in the same system (Figure 4). Thus,  $\text{NH}_4^+\text{-N}$  is efficiently oxidized and transformed to  $\text{NO}_2^-\text{-N}$  by *Nitrosomonadales*-like AOB in the upper part, and  $\text{NO}_2^-\text{-N}$  is oxidized and transformed to  $\text{NO}_3^-\text{-N}$  by *Nitrospirales*-like NOB in the middle to lower part. In addition, *Nitrobacter*-like NOB (Order; *Rhizobiales*) might be responsible for  $\text{NO}_2^-$  oxidation in the reactor, because *Rhizobiales* (2.8–6.3% of all orders) was detected in the reactor. The coexistence of AOB and NOB has been reported for various environments [38,39], wastewater treatment plants [40–42], and drinking water treatment plants [43]. AOB and NOB function independently, but their synergistic relationships mutually benefit their growth and activity [44]. AOB and NOB are in close proximity within biofilms, but the active  $\text{NH}_4^+$ -oxidizing zone is separate from the  $\text{NO}_2^-$ -oxidizing

zone at the micrometer colony diameter scale [45]. In the present study, we demonstrated that  $\text{NH}_4^+$  and  $\text{NO}_2^-$  oxidation in the nitrification unit treating contaminated groundwater was distinctly and widely separated from the top to the bottom of the flow.

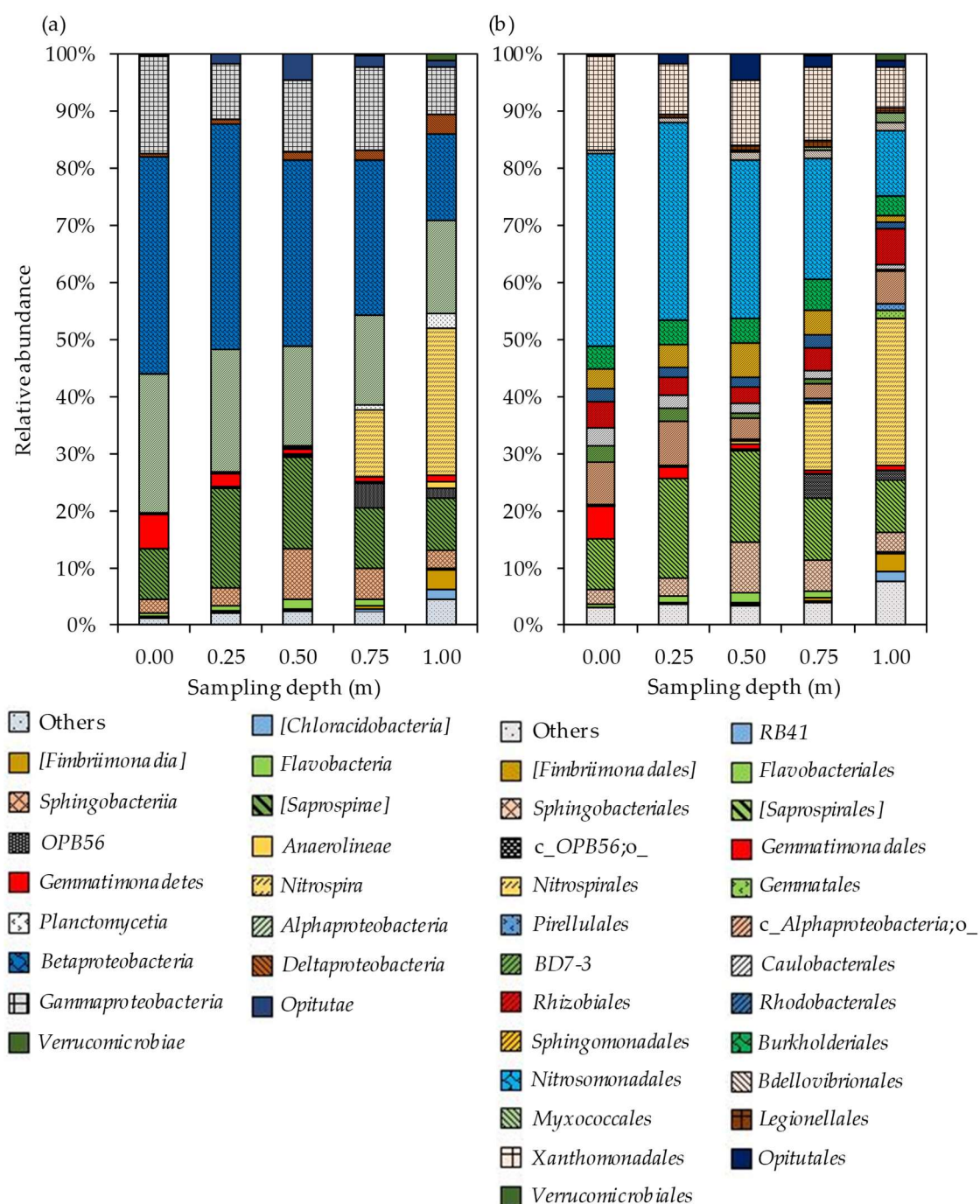


**Figure 6.** Bacterial community structures at the class (a) and order (b) levels along the single axis of the dropping flow on the 56th day of operation.

This study demonstrated the highly efficient  $\text{NH}_4^+$ -N removal from groundwater by using the dropping nitrification reactor and revealed the characteristics of the reactor for the first time. In future studies, we will examine the  $\text{NH}_4^+$ -N oxidation efficiency of the reactors in series and the operational lifetime of the sponge media. However,  $\text{NO}_2^-$ -N and  $\text{NO}_3^-$ -N were accumulated in the effluent of the reactor. Excess  $\text{NO}_3^-$ -N ( $>11 \text{ mg L}^{-1}$  for drinking water [10]) has a negative impact on human

health; thus, the effluent is still not recommended for drinking purposes. Therefore, we plan to conduct another study of  $\text{NH}_4^+$ -N removal from groundwater by combining nitrification with a denitrification or anammox system for complete nitrogen removal.

#### 4. Conclusions

The dropping nitrification reactor consisting of polyolefin sponge hanging units treated synthetic groundwater containing  $50 \text{ mg L}^{-1}$   $\text{NH}_4^+$ -N over 56 days at a flow rate of  $4.32 \text{ L day}^{-1}$ . The groundwater was aerated with atmospheric oxygen as it flowed downwards from the top to the bottom of the units. The reactor removed 50.8–68.7% of the  $\text{NH}_4^+$ -N. *Nitrosomonadales*-like AOB predominated in the upper part of the reactor and transformed  $\text{NH}_4^+$ -N to  $\text{NO}_2^-$ -N. *Nitrospirales*-like NOB predominated in the lower part of the reactor and transformed  $\text{NO}_2^-$ -N to  $\text{NO}_3^-$ -N. The dropping nitrification reactor is a promising technology for the removal of  $\text{NH}_4^+$ -N from contaminated groundwater.

**Supplementary Materials:** The following are available online at <http://www.mdpi.com/2073-4441/12/2/599/s1>, Figure S1: Schematic diagram of a dropping nitrification reactor, Figure S2: Zero-order (a) and first-order (b) kinetics for the decrease in  $\text{NH}_4^+$ -N along the single axis of the dropping nitrification units.  $\text{NH}_4^+$ -N concentrations represent the mean of four replicate reactors at different sampling depths. Comparison of the coefficients of determination ( $R^2$ ) between the zero- and first-order kinetic reactions (c), Table S1: Target genes for qPCR analysis, primers and sequences, annealing temperatures, and amplification sizes.

**Author Contributions:** All the authors conceived of the study design. A.K.M. performed the experiments, interpreted the results, and prepared a draft of the manuscript. T.T. checked and interpreted the results and corrected the draft of the manuscript. T.K., I.M.A., K.M., and F.K. discussed the results and critically reviewed the manuscript. All authors have read and agreed to the published version of the manuscript.

**Funding:** This research received no external funding.

**Acknowledgments:** This study was a part of the Science and Technology Research Partnership for Sustainable Development (SATREPS) project of the Japan International Cooperation Agency (JICA) and the Japan Science and Technology Agency (JST), titled “Project for Hydro-Microbiological Approach for Water Security in Kathmandu Valley, Nepal”.

**Conflicts of Interest:** The authors declare no conflicts of interest.

#### References

1. Shen, S.; Ma, T.; Du, Y.; Luo, K.; Deng, Y.; Lu, Z. Temporal variations in groundwater nitrogen under intensive groundwater/surface-water interaction. *Hydrogeol. J.* **2019**, *27*, 1753–1766. [CrossRef]
2. Siczka, A.; Koda, E. Kinetic and equilibrium studies of sorption of ammonium in the soil-water environment in agricultural areas of Central Poland. *Appl. Sci.* **2016**, *6*, 269. [CrossRef]
3. Vocciant, M.; De Folly D’Auris, A.; Finocchi, A.; Tagliabue, M.; Bellettato, M.; Ferrucci, A.; Reverberi, A.P.; Ferro, S. Adsorption of ammonium on clinoptilolite in presence of competing cations: Investigation on groundwater remediation. *J. Clean. Prod.* **2018**, *198*, 480–487. [CrossRef]
4. Siczka, A.; Bujakowski, F.; Falkowski, T.; Koda, E. Morphogenesis of a floodplain as a criterion for assessing the susceptibility to water pollution in an agriculturally rich valley of a lowland river. *Water* **2018**, *10*, 399. [CrossRef]
5. Malla, R.; Shrestha, S.; Chapagain, S.K.; Shakya, M.; Nakamura, T. Physico-chemical and oxygen-hydrogen isotopic assessment of Bagmati and Bishnumati rivers and the shallow groundwater along the river corridors in Kathmandu Valley, Nepal. *J. Water Resour. Prot.* **2015**, *7*, 1435–1448. [CrossRef]
6. Patterson, B.M.; Grassi, M.E.; Davis, G.B.; Robertson, B.S.; McKinley, A.J. Use of polymer mats in series for sequential reactive barrier remediation of ammonium-contaminated groundwater: Laboratory column evaluation. *Environ. Sci. Technol.* **2002**, *36*, 3439–3445. [CrossRef]
7. Lindenbaum, J. Identification of Sources of Ammonium in Groundwater Using Stable Nitrogen and Boron Isotopes in Nam Du, Hanoi. Master’s Thesis, Lund University, Lund, Sweden, 2012.
8. Huang, G.; Liu, F.; Yang, Y.; Kong, X.; Li, S.; Zhang, Y.; Cao, D. Ammonium-nitrogen-contaminated groundwater remediation by a sequential three-zone permeable reactive barrier (multibarrier) with oxygen-releasing compound (ORC)/clinoptilolite/spongy iron: Column studies. *Environ. Sci. Pollut. Res.* **2015**, *22*, 3705–3714. [CrossRef]

9. Chapagain, S.K.; Kazama, F. Overview of chemical quality of groundwater in the Kathmandu Valley. In *Kathmandu Valley Groundwater Outlook*; Shrestha, S., Pradhananga, D., Pandey, V.P., Eds.; Asian Institute of Technology (AIT), The Small Earth Nepal (SEN), Center of Research for Environment Energy and Water (CREEW), International Research Center for River Basin Environment-University of Yamanashi (ICRE-UY): Kathmandu, Nepal, 2012; pp. 49–55.
10. WHO. *Guidelines for Drinking-Water Quality*, 4th ed.; World Health Organization: Geneva, Switzerland, 2011.
11. Huang, G.; Liu, F.; Yang, Y.; Deng, W.; Li, S.; Huang, Y.; Kong, X. Removal of ammonium-nitrogen from groundwater using a fully passive permeable reactive barrier with oxygen-releasing compound and clinoptilolite. *J. Environ. Manag.* **2015**, *154*, 1–7. [[CrossRef](#)]
12. Li, S.; Huang, G.; Kong, X.; Yang, Y.; Liu, F.; Hou, G.; Chen, H. Ammonium removal from groundwater using a zeolite permeable reactive barrier: A pilot-scale demonstration. *Water Sci. Technol.* **2014**, *70*, 1540–1547. [[CrossRef](#)]
13. Patterson, B.M.; Grassi, M.E.; Robertson, B.S.; Davis, G.B.; Smith, A.J.; Mckinley, A.J. Use of polymer mats in series for sequential reactive barrier remediation of ammonium-contaminated groundwater: Field evaluation. *Environ. Sci. Technol.* **2004**, *38*, 6846–6854. [[CrossRef](#)]
14. Obiri-Nyarko, F.; Grajales-Mesa, S.J.; Malina, G. An overview of permeable reactive barriers for in situ sustainable groundwater remediation. *Chemosphere* **2014**, *111*, 243–259. [[CrossRef](#)] [[PubMed](#)]
15. Uemura, S.; Harada, H. Application of UASB technology for sewage treatment with a novel post-treatment process. In *Environmental Anaerobic Technology, Applications and New Developments*; Fang, H.H.P., Ed.; Imperial College Press: London, UK, 2010; pp. 91–112. [[CrossRef](#)]
16. Machdar, I.; Harada, H.; Ohashi, A.; Sekiguchi, Y.; Okui, H.; Ueki, K. A novel and cost-effective sewage treatment system consisting of UASB pre-treatment and aerobic post-treatment units for developing countries. *Water Sci. Technol.* **1997**, *36*, 189–197. [[CrossRef](#)]
17. Tawfik, A.; Ohashi, A.; Harada, H. Sewage treatment in a combined up-flow anaerobic sludge blanket (UASB)-down-flow hanging sponge (DHS) system. *Biochem. Eng. J.* **2006**, *29*, 210–219. [[CrossRef](#)]
18. Okubo, T.; Onodera, T.; Uemura, S.; Yamaguchi, T.; Ohashi, A.; Harada, H. On-site evaluation of the performance of a full-scale down-flow hanging sponge reactor as a post-treatment process of an up-flow anaerobic sludge blanket reactor for treating sewage in India. *Bioresour. Technol.* **2015**, *194*, 156–164. [[CrossRef](#)] [[PubMed](#)]
19. Onodera, T.; Okubo, T.; Uemura, S.; Yamaguchi, T.; Ohashi, A.; Harada, H. Long-term performance evaluation of down-flow hanging sponge reactor regarding nitrification in a full-scale experiment in India. *Bioresour. Technol.* **2016**, *204*, 177–184. [[CrossRef](#)] [[PubMed](#)]
20. Onodera, T.; Tandukar, M.; Sugiyana, D.; Uemura, S.; Ohashi, A.; Harada, H. Development of a sixth-generation down-flow hanging sponge (DHS) reactor using rigid sponge media for post-treatment of UASB treating municipal sewage. *Bioresour. Technol.* **2014**, *152*, 93–100. [[CrossRef](#)]
21. Hatamoto, M.; Okubo, T.; Kubota, K.; Yamaguchi, T. Characterization of downflow hanging sponge reactors with regard to structure, process function, and microbial community compositions. *Appl. Microbiol. Biotechnol.* **2018**, *102*, 10345–10352. [[CrossRef](#)]
22. Araki, N.; Ohashi, A.; Machdar, I.; Harada, H. Behaviors of nitrifiers in a novel biofilm reactor employing hanging sponge-cubes as attachment site. *Water Sci. Technol.* **1999**, *39*, 23–31. [[CrossRef](#)]
23. Tandukar, M.; Machdar, I.; Uemura, S.; Ohashi, A.; Harada, H. Potential of a combination of UASB and DHS reactor as a novel sewage treatment system for developing countries: Long-term evaluation. *J. Environ. Eng.* **2006**, *132*, 166–172. [[CrossRef](#)]
24. Khanitchaidecha, W.; Shakya, M.; Nakano, Y.; Tanaka, Y.; Kazama, F. Development of an attached growth reactor for NH<sub>4</sub>-N removal at a drinking water supply system in Kathmandu Valley, Nepal. *J. Environ. Sci. Heal.-Part A Toxic/Hazardous Subst. Environ. Eng.* **2012**, *47*, 734–743. [[CrossRef](#)]
25. APHA; AWWA; WEF. *Standard Methods for the Examination of Water and Wastewater*, 20th ed.; Clesceri, L.S., Greenberg, A.E., Eaton, A.D., Eds.; American Public Health Association, American Water Works Association, Water Environment Federation: Washington, DC, USA, 1998.
26. Richardson, D.J.; Watmough, N.J. Inorganic nitrogen metabolism in bacteria. *Curr. Opin. Chem. Biol.* **1999**, *3*, 207–219. [[CrossRef](#)]

27. Schmidt, I.; Sliemers, O.; Schmid, M.; Bock, E.; Fuerst, J.; Kuenen, J.G.; Jetten, M.S.M.; Strous, M. New concepts of microbial treatment processes for the nitrogen removal in wastewater. *FEMS Microbiol. Rev.* **2003**, *27*, 481–492. [[CrossRef](#)]
28. Machdar, I.; Muhammad, S.; Onodera, T.; Syutsubo, K. A pilot-scale study on a down-flow hanging sponge reactor for septic tank sludge treatment. *Environ. Eng. Res.* **2018**, *23*, 195–204. [[CrossRef](#)]
29. Okubo, T.; Kubota, K.; Yamaguchi, T.; Uemura, S.; Harada, H. Development of a new non-aeration-based sewage treatment technology: Performance evaluation of a full-scale down-flow hanging sponge reactor employing third-generation sponge carriers. *Water Res.* **2016**, *102*, 138–146. [[CrossRef](#)]
30. Vymazal, J. Removal of nutrients in various types of constructed wetlands. *Sci. Total Environ.* **2007**, *380*, 48–65. [[CrossRef](#)]
31. Hooper, A.B.; Vannelli, T.; Bergmann, D.J.; Arciero, D.M. Enzymology of the oxidation of ammonia to nitrite by bacteria. *Antonie Van Leeuwenhoek* **1997**, *71*, 59–67. [[CrossRef](#)]
32. Hagopian, D.S.; Riley, J.G. A closer look at the bacteriology of nitrification. *Aquac. Eng.* **1998**, *18*, 223–244. [[CrossRef](#)]
33. Li, B.; Irvin, S.; Baker, K. The variation of nitrifying bacterial population sizes in a sequencing batch reactor (SBR) treating low, mid, high concentrated synthetic wastewater. *J. Environ. Eng. Sci.* **2007**, *6*, 651–663. [[CrossRef](#)]
34. You, S.J.; Hsu, C.L.; Chuang, S.H.; Ouyang, C.F. Nitrification efficiency and nitrifying bacteria abundance in combined AS-RBC and A2O systems. *Water Res.* **2003**, *37*, 2281–2290. [[CrossRef](#)]
35. Ward, B. Nitrification. *Encycl. Ecol.* **2013**, *2*, 351–358. [[CrossRef](#)]
36. Yao, Q.; Peng, D.C. Nitrite oxidizing bacteria (NOB) dominating in nitrifying community in full-scale biological nutrient removal wastewater treatment plants. *AMB Express* **2017**, *7*, 1–11. [[CrossRef](#)] [[PubMed](#)]
37. Kubota, K.; Hayashi, M.; Matsunaga, K.; Iguchi, A.; Ohashi, A.; Li, Y.Y.; Yamaguchi, T.; Harada, H. Microbial community composition of a down-flow hanging sponge (DHS) reactor combined with an up-flow anaerobic sludge blanket (UASB) reactor for the treatment of municipal sewage. *Bioresour. Technol.* **2014**, *151*, 144–150. [[CrossRef](#)] [[PubMed](#)]
38. Cébron, A.; Garnier, J. *Nitrobacter* and *Nitrospira* genera as representatives of nitrite-oxidizing bacteria: Detection, quantification and growth along the lower Seine River (France). *Water Res.* **2005**, *39*, 4979–4992. [[CrossRef](#)] [[PubMed](#)]
39. Okabe, S.; Nakamura, Y.; Satoh, H. Community structure and in situ activity of nitrifying bacteria in *Phragmites* root-associated biofilms. *Microbes Environ.* **2012**, *27*, 242–249. [[CrossRef](#)]
40. Gieseke, A.; Nielsen, J.L.; Amann, R.; Nielsen, P.H.; De Beer, D. In situ substrate conversion and assimilation by nitrifying bacteria in a model biofilm. *Environ. Microbiol.* **2005**, *7*, 1392–1404. [[CrossRef](#)]
41. Larsen, P.; Nielsen, J.L.; Svendsen, T.C.; Nielsen, P.H. Adhesion characteristics of nitrifying bacteria in activated sludge. *Water Res.* **2008**, *42*, 2814–2826. [[CrossRef](#)]
42. Siripong, S.; Rittmann, B.E. Diversity study of nitrifying bacteria in full-scale municipal wastewater treatment plants. *Water Res.* **2007**, *41*, 1110–1120. [[CrossRef](#)]
43. Liu, Y.; Liu, C.; Nelson, W.C.; Shi, L.; Xu, F.; Liu, Y.; Yan, A.; Zhong, L.; Thompson, C.; Fredrickson, J.K.; et al. Effect of water chemistry and hydrodynamics on nitrogen transformation activity and microbial community functional potential in hyporheic zone sediment columns. *Environ. Sci. Technol.* **2017**, *51*, 4877–4886. [[CrossRef](#)]
44. Cai, M.; Ng, S.-K.; Lim, C.K.; Lu, H.; Jia, Y.; Lee, P.K.H. Physiological and metagenomic characterizations of the synergistic relationships between ammonia- and nitrite-oxidizing bacteria in freshwater nitrification. *Front. Microbiol.* **2018**, *9*, 1–13. [[CrossRef](#)]
45. Okabe, S.; Satoh, H.; Watanabe, Y. In situ analysis of nitrifying biofilms as determined by in situ hybridization and the use of microelectrodes. *Appl. Environ. Microbiol.* **1999**, *65*, 3182–3191. [[CrossRef](#)]

